Convergence behaviour of Dirichlet–Neumann and Robin methods for a nonlinear transmission problem

Heiko Berninger, Ralf Kornhuber, and Oliver Sander*

Fachbereich Mathematik und Informatik, Freie Universität Berlin

Summary. We investigate Dirichlet–Neumann and Robin methods for a quasilinear elliptic transmission problem in which the nonlinearity changes discontinuously across two subdomains. In one space dimension we obtain convergence theorems by extending known results from the linear case. They hold both on the continuous and on the discrete level. From the proofs one can infer mesh-independence of the convergence rates for the Dirichlet–Neumann method, but not for the Robin method. In two space dimensions we consider numerical examples which demonstrate that the theoretical results might be extended to higher dimensions. Moreover, we investigate the asymptotic convergence behaviour for fine mesh sizes quantitatively. We observe a good agreement with many known linear results, which is remarkable in view of the nonlinear character of the problem.

1 Introduction

We consider the following setting. Let $\Omega \subset \mathbb{R}^n$ be a bounded Lipschitz domain divided into two non-overlapping subdomains Ω_1, Ω_2 with the interface $\Gamma = \overline{\Omega}_1 \cap \overline{\Omega}_2$. The outer normal of Ω_1 is denoted by $\mathbf{n}$. Furthermore, let $f \in L^2(\Omega)$ and k_1, $k_2 \in L^\infty(\mathbb{R})$ with $k_i \geq \alpha > 0$ for $i = 1, 2$. In strong form the domain decomposition problem that we aim at reads:

Find a function p in Ω, $p_i := p_{|\Omega_i} \in H^1(\Omega_i)$, $i = 1, 2$, $p_{|\partial\Omega} = 0$, such that

$$-\operatorname{div}(k_i(p_i)\nabla p_i) = f \qquad \text{on } \Omega_i, \ \ i = 1, 2 \tag{1}$$

$$p_1 = p_2 \qquad \text{on } \Gamma \tag{2}$$

$$k_1(p_1)\nabla p_1 \cdot \mathbf{n} = k_2(p_2)\nabla p_2 \cdot \mathbf{n} \qquad \text{on } \Gamma\,. \tag{3}$$

A powerful tool to treat problems of this kind is to introduce new variables u_i, $i = 1, 2$, by Kirchhoff transformations κ_i, defined by

* This work was supported by the BMBF–Programm "Mathematik für Innovationen in Industrie und Dienstleistungen". We thank J. Schreiber for computational assistence.

$$u_i(x) := \kappa_i(p_i(x)) = \int_0^{p_i(x)} k_i(q)\,dq \quad \text{a.e. in } \Omega_i\,. \tag{4}$$

This entails $k_i(p_i)\nabla p_i = \nabla u_i$ and, therefore, problem (1)–(3) can be rewritten in the following form, in which the nonlinearity only appears on Γ, but now as a discontinuity condition on the primal variable.

Find a function u in Ω, $u_i := u_{|\Omega_i} \in H^1(\Omega_i)$, $i = 1, 2$, $u_{|\partial\Omega} = 0$, such that

$$-\Delta u_i = f \qquad \text{on } \Omega_i,\ \ i = 1, 2 \tag{5}$$

$$\kappa_1^{-1}(u_1) = \kappa_2^{-1}(u_2) \qquad \text{on } \Gamma \tag{6}$$

$$\nabla u_1 \cdot \mathbf{n} = \nabla u_2 \cdot \mathbf{n} \qquad \text{on } \Gamma\,. \tag{7}$$

In the linear case, where k_i, $i = 1, 2$, are constant functions, Dirichlet–Neumann and Robin methods are well-understood iteration procedures for the treatment of non-overlapping elliptic domain decomposition problems, see, e.g., [8], [10] and [7]. We introduce nonlinear versions of these methods applied to (5)–(7) without using linearization. In one space dimension, both on the continuous and on the discrete level, we obtain convergence results by extending approaches used in the linear case, see [1]. We also obtain mesh-independent convergence rates for the damped Dirichlet–Neumann method, but not for the Robin method, just as in the linear case. However, these generalizations of the convergence proofs for the linear setting do not work in dimensions higher than one. Therefore, we investigate the qualitative and quantitative convergence properties in 2D numerically.

Concerning the nonlinear Dirichlet–Neumann method, we observe asymptotically mesh-independent optimal convergence rates for a certain mesh-independent optimal damping parameter. Moreover, if the nonlinearities k_1 and k_2 are of different orders of magnitude, the Dirichlet–Neumann method converges considerably faster than if they are of the same order of magnitude. Strangely enough, this observation can be made plausible by investigations that have been carried out on corresponding settings for the Robin method in the linear case, see [5].

As to the nonlinear Robin method, we observe degenerating optimal convergence rates and parameters if the two Robin parameters involved in the method coincide. What is more, we can even establish formulas, which quantitatively describe the asymptotic behaviour of this degeneracy, and which are very similar to the ones, that have been discovered for the Robin method applied to the linear case, cf. [9]. Results from the theory of optimized Schwarz methods in linear cases (see, e.g., [7]) show, that the convergence speed can be further increased by allowing the two Robin parameters to be different. Indeed, we obtain a better asymptotic behaviour for our test cases if we choose the parameters independently from each other. Finally, if the nonlinearities k_1 and k_2 are of different orders of magnitude, the optimized Robin method with different parameters converges quite fast with mesh-independent convergence rates, which, again, reproduces the linear situation as considered in [5].

Altogether, the observations we make in our nonlinear numerical examples, resemble strikingly well the proved results for linear cases.

2 Transmission problem with jumping nonlinearities

In this section we introduce some further notation (cf. [10]) and give a weak formulation of problem (5)–(7). Then, we point out the equivalence of it with Steklov–Poincaré interface equations (cf. [3]).

In addition to the notation and definitions above we introduce the spaces

$$V_i := \{v_i \in H^1(\Omega_i) \,|\, v_{i|\partial\Omega\cap\partial\Omega_i} = 0\}, \quad V_i^0 := H_0^1(\Omega_i), \quad \Lambda := H_{00}^{1/2}(\Gamma)$$

and for $w_i, v_i \in V_i$ the form $a_i(w_i, v_i) := (\nabla w_i, \nabla v_i)_{\Omega_i}$, where $(\cdot,\cdot)_{\Omega_i}$ stands for the L^2 inner product on Ω_i. The norm in Λ will be denoted by $\|\cdot\|_\Lambda$.

Let R_i, $i = 1, 2$, be any continuous extension operator from Λ to V_i. Then the variational formulation of problem (5)–(7) reads as follows:

Find $u_i \in V_i$, $i = 1, 2$, such that

$$a_i(u_i, v_i) = (f, v_i)_{\Omega_i} \qquad \forall v_i \in V_i^0, \;\; i = 1, 2 \tag{8}$$

$$\kappa_1^{-1}(u_{1|\Gamma}) = \kappa_2^{-1}(u_{2|\Gamma}) \qquad \text{in } \Lambda \tag{9}$$

$$a_1(u_1, R_1\mu) - (f, R_1\mu)_{\Omega_1} = -a_2(u_2, R_2\mu) + (f, R_2\mu)_{\Omega_2} \quad \forall \mu \in \Lambda\,. \tag{10}$$

For details concerning the Kirchhoff transformations in the weak sense in (9), i.e., in the sense of superposition operators on $H^1(\Omega_i)$, see [2], where one can also find a proof of

Proposition 1. *The weak form of problem (1)–(3) is equivalent to (8)–(10).*

Now, for a given $\lambda \in \Lambda$ (and omitting brackets for operators applied to λ from now on), we consider the harmonic extensions $H_i(\kappa_i\lambda) \in V_i$ of the Dirichlet boundary value $\kappa_i\lambda$ on Γ for $i = 1, 2$. With these operators and denoting by $\langle\cdot,\cdot\rangle$ the duality pairing between Λ' and Λ, we recall that the Steklov–Poincaré operators $S_i : \Lambda \to \Lambda'$ are defined by

$$\langle S_i\eta, \mu\rangle = a_i(H_i\eta, H_i\mu) \quad \forall \eta, \mu \in \Lambda\,, \quad i = 1, 2\,.$$

Furthermore, let $\mathcal{G}_i f$ be the solutions of the subproblems (8) with homogeneous Dirichlet data $(\mathcal{G}_i f)_{|\partial\Omega_i} = 0$. We define the functional $\chi = \chi_1 + \chi_2 \in \Lambda'$ by

$$\langle\chi_i, \mu\rangle = (f, H_i\mu)_{\Omega_i} - a_i(\mathcal{G}_i f, H_i\mu) \quad \forall \mu \in \Lambda\,, \quad i = 1, 2\,.$$

Proposition 2. *By (4) and the relation*

$$u_i = H_i\kappa_i\lambda + \mathcal{G}_i f\,, \quad i = 1, 2\,, \tag{11}$$

between λ and u_i as well as with $\lambda_2 = \kappa_2\lambda$, problem (8)–(10) is equivalent to each of the two Steklov–Poincaré interface equations

$$\textit{find } \lambda \in \Lambda: \qquad (S_1\kappa_1 + S_2\kappa_2)\lambda = \chi\,, \tag{12}$$

$$\textit{find } \lambda_2 \in \Lambda: \qquad (S_1\kappa_1\kappa_2^{-1} + S_2)\lambda_2 = \chi\,. \tag{13}$$

3 Nonlinear Dirichlet–Neumann and Robin methods

In this section we note the nonlinear Dirichlet–Neumann and Robin methods that we apply to (8)–(10) in weak forms. We give Steklov–Poincaré formulations of the methods and convergence results in 1D generalizing linear theory.

3.1 The methods and their Steklov–Poincaré formulations

The nonlinear Dirichlet–Neumann method applied to problem (8)–(10) reads:
Given $\lambda_2^0 \in \Lambda$, find $u_1^{k+1} \in V_1$ and $u_2^{k+1} \in V_2$ for each $k \geq 0$ such that

$$a_1(u_1^{k+1}, v_1) = (f, v_1)_{\Omega_1} \qquad \forall v_1 \in V_1^0 \tag{14}$$

$$u_{1|\Gamma}^{k+1} = \kappa_1 \kappa_2^{-1}(\lambda_2^k) \qquad \text{in } \Lambda \tag{15}$$

and then

$$a_2(u_2^{k+1}, v_2) = (f, v_2)_{\Omega_2} \qquad \forall v_2 \in V_2^0 \tag{16}$$

$$a_2(u_2^{k+1}, H_2\mu) - (f, H_2\mu)_{\Omega_2} = -a_1(u_1^{k+1}, H_1\mu) + (f, H_1\mu)_{\Omega_1} \quad \forall \mu \in \Lambda\,. \tag{17}$$

Then, with some damping parameter $\theta \in (0, 1)$, the new iterate is defined by

$$\lambda_2^{k+1} := \theta\, u_{2|\Gamma}^{k+1} + (1-\theta)\lambda_2^k\,. \tag{18}$$

For the analysis (cf. [1, Sec. 3.3.2/3]), it is necessary to carry out the damping in the transformed space and to have a linear preconditioner in

Proposition 3. *The Dirichlet–Neumann method (14)–(18) applied to problem (8)–(10) is a* preconditioned Richardson procedure *for equation (13) with S_2 as a preconditioner. The iteration is given by $T_\theta : \Lambda \to \Lambda$ defined as*

$$T_\theta : \lambda_2^k \mapsto \lambda_2^{k+1} = \lambda_2^k + \theta S_2^{-1}(\chi - (S_1\kappa_1\kappa_2^{-1} + S_2)\lambda_2^k)\,. \tag{19}$$

In contrast to the Dirichlet–Neumann method, the Robin iteration is related to the symmetric equation (12), and it comes with two acceleration parameters γ_1, $\gamma_2 > 0$ rather than one. For problem (8)–(10) it reads:
Given a $u_2^0 \in V_2$ find $u_1^{k+1} \in V_1$ and $u_2^{k+2} \in V_2$ for $k \geq 0$ such that

$$a_1(u_1^{k+1}, v_1) = (f, v_1)_{\Omega_1} \quad \forall v_1 \in V_1^0 \tag{20}$$

$$\begin{aligned} a_1(u_1^{k+1}, R_1\mu) - (f, R_1\mu)_{\Omega_1} + \gamma_1(\kappa_1^{-1}u_1^{k+1}, \mu)_\Gamma = \\ - a_2(u_2^k, R_2\mu) + (f, R_2\mu)_{\Omega_2} + \gamma_1(\kappa_2^{-1}u_2^k, \mu)_\Gamma \quad \forall \mu \in \Lambda \end{aligned} \tag{21}$$

and then

$$a_2(u_2^{k+1}, v_2) = (f, v_2)_{\Omega_2} \quad \forall v_2 \in V_2^0 \tag{22}$$

$$\begin{aligned} a_2(u_2^{k+1}, R_2\mu) - (f, R_2\mu)_{\Omega_1} + \gamma_2(\kappa_2^{-1}u_2^{k+1}, \mu)_\Gamma = \\ - a_1(u_1^{k+1}, R_1\mu) + (f, R_1\mu)_{\Omega_1} + \gamma_2(\kappa_1^{-1}u_1^{k+1}, \mu)_\Gamma \quad \forall \mu \in \Lambda\,. \end{aligned} \tag{23}$$

With the notation

$$\langle I\eta, \mu\rangle = (\eta, \mu)_\Gamma \quad \forall \eta, \mu \in \Lambda\,. \tag{24}$$

we obtain the following formulation of the Robin method in terms of Steklov–Poincaré operators (cf. [1, Sec. 3.4.2]), generalizing linear theory in [4, Sec. 5.4].

Proposition 4. *The Robin iteration (20)–(23) applied to (8)–(10) is equivalent to the* Alternating Direction Iterative (ADI) method *applied to (12). With a given $\lambda_2^0 \in \Lambda$ the operator $T_{\gamma_1,\gamma_2} : \Lambda \to \Lambda$, $T_{\gamma_1,\gamma_2} : \lambda_2^k \mapsto \lambda_2^{k+1}$ providing the ADI method is given by*

$$\lambda_2^{k+1} = (\gamma_2 I + S_2\kappa_2)^{-1}(\chi + (\gamma_2 I - S_1\kappa_1)(\gamma_1 I + S_1\kappa_1)^{-1}(\chi + (\gamma_1 I - S_2\kappa_2)\lambda_2^k))\,.$$

3.2 Convergence results

The approach for proving convergence is as follows, cf. [1]. First, a fixed point λ of the iterative scheme in Proposition 3 or 4 is a solution of (13) or (12), respectively. Secondly, convergence proofs for linear cases can be extended so that Banach's fixed point theorem can be applied to T_θ and T_{γ_1,γ_2}.

We give sufficient conditions for convergence which are almost the same for both methods. In case of the Dirichlet–Neumann method they entail that T_θ is a contraction if θ is small enough, so that we obtain mesh-independent convergence rates. This is not provided by the convergence proof for the Robin method, and, even in linear cases, it is not true for the Robin iteration.

Generalizing [10, pp. 118/9] for the Dirichlet–Neumann method we obtain

Theorem 1. *Let β_2 be the Lipschitz and α_2 be the coercivity constant of S_2. Let $S_1\kappa_1\kappa_2^{-1}$ be Lipschitz continuous with Lipschitz constant β_1 such strongly monotone with monotonicity constant α_1. Then (13) has a unique solution $\lambda_2 \in \Lambda$. Furthermore, for any given $\lambda_2^0 \in \Lambda$ and any $\theta \in (0, \theta_{\max})$ with $\theta_{\max}$ as in (25) the sequence given by (19) converges in Λ to λ_2. Theoretically optimal (i.e., minimal) convergence rates ρ_{opt} for corresponding optimal damping parameters θ_{opt} are given by*

$$\theta_{opt} = \frac{\theta_{\max}}{2} = \frac{\alpha_1+\alpha_2}{(\beta_1+\beta_2)^2}\cdot\frac{\alpha_2^2}{\beta_2} \quad \textit{and} \quad \rho_{opt} = 1 - \left(\frac{\alpha_1+\alpha_2}{\beta_1+\beta_2}\right)^2 \cdot \left(\frac{\alpha_2}{\beta_2}\right)^2\,. \tag{25}$$

Theorem 2. *The assumptions in Theorem 1 are satisfied in 1D.*

We do not know whether the assertion of Theorem 1 is true for higher dimensions. We remark, however, that there are operators $S_1\kappa_1\kappa_2^{-1} : \Lambda \to \Lambda'$ in 2D, that are not monotone, see [1, Sec. 3.3.4].

Theorem 3. *We assume that the problems in (8) and (10) are discretized by piecewise linear finite elements and that in (9) piecewise linear interpolation is applied to the function after having been Kirchhoff–transformed in the nodes of the interface. Then Theorem 1 can also be applied to this discretization with the same constants and, thus, leads to mesh-independent optimal convergence rates and optimal damping parameters.*

For proving convergence of the Robin method (generalizing the linear result in [4, pp. 99/100]) we need $S_1\kappa_1, S_2\kappa_2 : \Lambda \to \Lambda'$ to be Lipschitz continuous and strongly monotone, which, by Theorem 2, is satisfied in 1D.

Theorem 4. *Let $\gamma_1 = \gamma_2 = \gamma > 0$ and $\Omega \subset \mathbb{R}$. Then for any initial iterate $\lambda_2^0 \in \Lambda$ the operator $\mathcal{T}_\gamma = \mathcal{T}_{\gamma_1,\gamma_2}$ in Proposition 4 provides a sequence $(\lambda_2^k)_{k\geq 0}$ which converges in Λ to the unique fixed point of $\mathcal{T}_\gamma$. Moreover, the sequence $(u_i^k)_{k\geq 1}$, $i = 1, 2$, of Robin iterates converges to the solution of (8)–(10).*

For the discretization of problem (8)–(10) in Theorem 3 the corresponding discrete version of the Robin method converges to the discrete solution.

4 Parameter studies for the Dirichlet–Neumann method

The purpose of this section is to apply our nonlinear Dirichlet–Neumann method (14)–(18) to two concretely specified cases of the transmission problem in two space dimensions, discretized as in Theorem 3. After a detailed description of these two examples we present the numerical results which we discuss and compare to the linear case.

We consider problem (1)–(3) on the unit Yin Yang domain Ω within a circle of radius 1 as shown in Figure 1, with the coarse grid. We denote the white subdomain together with the grey circle B_1 by Ω_1 and the grey subdomain with the white circle B_2 by Ω_2. Furthermore, we select data f on Ω with $f_{|B_i} = f_i$ vanishing outside $B_1 \cup B_2$ and nonlinearities

$$k_i(p_i) = \begin{cases} K_i\, p_{b,i} \max\{(-p_i)^{-3\lambda_i - 2},\, c\} & \text{for } p_i \leq -1 \\ 1 & \text{for } p_i \geq -1 \end{cases} \tag{26}$$

with parameters $K_i, p_{b,i}, \lambda_i$ specified in Tables 1 and 2. The ellipticity constant $c > 0$ is supposed to enforce convergence.

Our choice represents a nondegenerate stationary Richards equation without gravity on Ω_1 and Ω_2 containing two different soil types. f_1 and f_2 can be regarded as a source and a sink. In Case I, which we call mildly heterogeneous, we only alter one soil parameter $\lambda_1 \neq \lambda_2$ and choose $p_{b,i} = -1.0$ and $K_i = 2.0 \cdot 10^{-3}$ in both subdomains Ω_i as well as $c = 0.1$. In Case II, which we refer to as strongly heterogeneous, we change all parameters and use $c = 0.01$.

Starting with the coarse grid (level 1) we apply uniform refinement in order to obtain finer meshes, i.e., higher (refinement) levels. We discretize (8)–(10)

	f_i	λ_i
$i = 1$	1.0	0.1
$i = 2$	-1.0	1.0

Table 1. Case I

	f_i	λ_i	$p_{b,i}$	K_i
$i = 1$	$5.0 \cdot 10^{-5}$	0.165	-0.373	$1.67 \cdot 10^{-7}$
$i = 2$	$-2.5 \cdot 10^{-3}$	0.694	-0.0726	$6.54 \cdot 10^{-5}$

Table 2. Case II

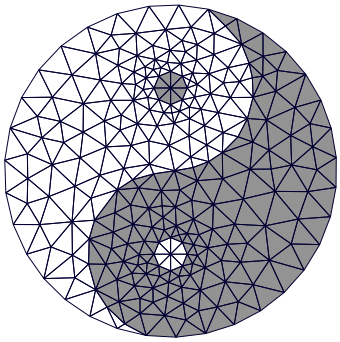

Fig. 1. Yin Yang domain Ω

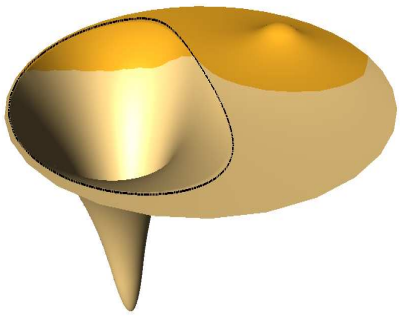

Fig. 2. Solution p on Ω in Case I (mildly heterogeneous)

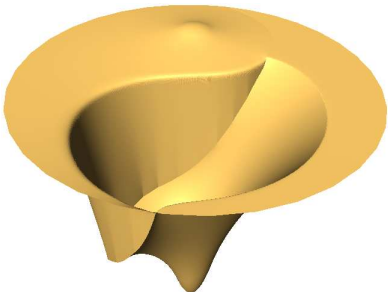

Fig. 3. Solution p on Ω in Case II (strongly heterogeneous)

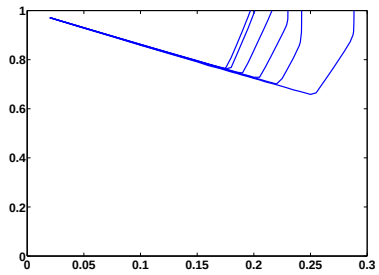

Fig. 4. ρ vs. θ on levels 1 (rightmost curve) to 6 (leftmost curve) in Case I

as described in Theorem 3. Figures 2 and 3 show the solutions p on Ω for the mildly and the strongly heterogeneous case, respectively. The crater-like parts of the graphs (indicated by a black line in Figure 2) correspond to the nonlinear (hydrologically, the unsaturated) regime of the equation.

For Case I, Figure 4 shows average convergence rates ρ of the Dirichlet–Neumann method with respect to the damping parameter θ on the first six levels, from the rightmost curve representing the first level to the leftmost curve corresponding to the 6th level. The convergence rates are measured in the energy norm for the transformed variables. Starting with the initial iterates $u_i^0 = 0$, $i = 1, 2$, the Dirichlet–Neumann iteration is stopped when the relative error is below 10^{-12}. Each of the local problems on the subdomains is solved by 50 iterations of a linear multigrid which leads to numerically exact solutions. For the implementation we used the numerics environment DUNE [6].

Figure 4 shows that, as on the continuous level in Theorem 1, one obtains convergence if the damping parameter $\theta \in (0, 1)$ is below a threshold $\theta_{\max}$, and one observes optimal convergence rates ρ_{opt} for a certain θ_{opt}. Both the

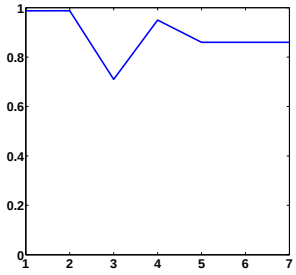

Fig. 5. θ_{opt} vs. level in Case II

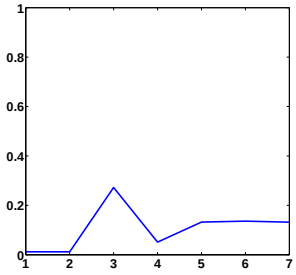

Fig. 6. ρ_{opt} vs. level in Case II

threshold and the optimal parameter as well as the corresponding optimal rates are level-dependent—however, these values seem to stabilize for higher levels. Concretely, the damping parameter $\theta_{opt} \approx 0.17$ leads to the optimal convergence rates $\rho_{opt} \approx 0.77$ on levels 5, 6 and 7. This indicates that mesh-independence is obtained in this 2D-case as was proved for 1D-cases (Theorem 3) and is known in linear settings (see [10, pp. 122–128]). Finally, we have the relationship $\rho_{opt} \approx 1 - \frac{7}{5}\theta_{opt}$ on all levels 1 to 7, which reflects (25).

In principle, the situation for Case II is the same as for Case I, see Figures 5 and 6. Again, optimal convergence rates corresponding to optimal damping parameters seem to stabilize asymptotically for high levels, but now we need considerably less damping $\theta_{opt} \approx 0.85$ for much better optimal rates $\rho_{opt} \approx 0.15$ (on levels 5, 6 and 7) than in Case I. In addition, even for overrelaxation, i.e. for parameters $\theta > 1$, convergence can be observed (concretely, we obtain $\theta_{opt} = \theta_{\max}/2$ as in (25)). In contrast to Case I, the convergence rates remain stable even if we choose a much smaller $c > 0$, e.g., $c = 10^{-100}$.

A possible reason for this considerably improved convergence behaviour of the Dirichlet–Neumann method might be the big jumps of the diffusion coefficients K_1 and K_2 in Case II. Surprisingly, the numerical results in the next section, where we present the convergence behaviour of the nonlinear Robin method for the two test cases, will shed some light on this phenomenon, again supported by linear theory. Here, we want to discuss this issue heuristically, regardless of the linear or nonlinear nature of the problem, by considering the corresponding constants in Theorem 1. Motivated by $K_1 \ll K_2$ in Table 2, we assume that $\alpha_2 \simeq \beta_2$ have the same order of magnitude which is "big" compared to $\alpha_1 \simeq \beta_1$. Then, considering (25), we estimate roughly

$$\rho_{opt} = 1 - \frac{\alpha_1 + \alpha_2}{\beta_2}\theta_{opt} \simeq 1 - \theta_{opt}$$

which, indeed, is the relation between θ_{opt} and ρ_{opt} on levels 1 to 7 displayed in Figures 5 and 6. With the same arguments we find that θ_{opt} has the order of magnitude of α_2. Indeed, if we exchange the Dirichlet-subdomain Ω_1 and the Neumann-subdomain Ω_2, we only obtain convergence for very small damp-

ing parameters in Case II, whereas we do hardly see any change in Case I. Also, the convergence rates are very bad for Case II after exchanging domains. This, however, cannot be inferred from the formula in (25), but by numerical stability: One can argue that the smaller K_1 is, the better the Dirichlet problem is conditioned on Ω_1 (with respect to the Dirichlet value), and the bigger K_2 is, the better the Neumann problem is conditioned on Ω_2 (with respect to the Neumann value). For more illuminating theory on linear cases with discontinuous coefficients, which confirms some of our findings in Case II, consult [5, p. 97]. Altogether, in such asymmetric cases, the asymmetry of the Dirichlet–Neumann method reveals itself dramatically.

5 Parameter studies for the Robin method

In this last section we present numerical results obtained by applying the nonlinear Robin method (20)–(23) to the test cases introduced in Section 4. For both cases we first consider the Robin method with one Robin parameter $\gamma = \gamma_1 = \gamma_2$, for which our convergence result (Theorem 4) in 1D is valid, and secondly, we investigate the situation with different γ_1 and γ_2. In contrast to the Dirichlet–Neumann method, each subproblem (20)–(21) and (22)–(23) in the Robin iteration is nonlinear. We solve these local problems by a monotone multigrid method, see [1, Sec. 3.4.5]. The latter is stopped if the relative error of succeeding iterates in the energy norm drops below 10^{-12}. Otherwise, we use the same stopping criterion and average convergence rates as for the Dirichlet–Neumann method above.

Using the Robin iteration with $\gamma = \gamma_1 = \gamma_2$, we find that the numerical results of the two cases are virtually the same. Therefore, we only present Case II here. As one can see in Figure 7, there are certain ranges for the Robin parameter γ on each level 1 to 6, where convergence rates are bounded away from 1. This is remarkable since Theorem 4 guarantees convergence for all $\gamma > 0$ in 1D. Furthermore—as for the Dirichlet–Neumann method—there is an optimal convergence rate ρ_{opt} obtained for an optimal γ_{opt} on each level. However—in contrast to the Dirichlet–Neumann method—these optimal rates and the corresponding parameters seem to degenerate rather than become asymptotically mesh-independent. The situation in Case I is almost the same as in Case II. However, the range of Robin parameters, for which an acceptable convergence speed is observed in the numerics, is about 10^4 times bigger than in Case II. Thus, a good choice of γ seems to be correlated to the factor in front of the Laplacian (compare (21)), which is by some orders of magnitude bigger in Case I than in Case II.

In convergence proofs for the Robin method on the continuous level, as in the original [8], one usually does not derive convergence rates (compare Section 3.2). This is because, usually, they are just not available. On the contrary, degeneracy of convergence rates is observed and proved on the discrete level for fine mesh sizes. In the world of optimized Schwarz methods, the latter can

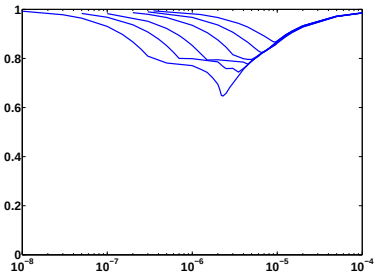

Fig. 7. ρ vs. γ on levels 1 (leftmost) to 6 (rightmost) for $\gamma_1 = \gamma_2$ in Case II

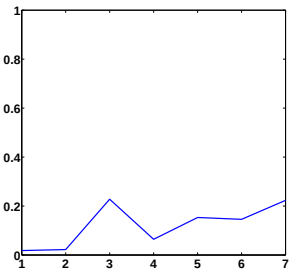

Fig. 8. ρ_{opt} vs. level for $\gamma_1 \neq \gamma_2$ in Case II

even be formulated quantitatively in form of asymptotic convergence results. For example, in linear cases the asymptotic behaviour

$$\gamma_{opt}^{lin} = \mathcal{O}(h^{-1/2}) \quad \text{and} \quad \rho_{opt}^{lin} = 1 - \mathcal{O}(h^{1/2}) \tag{27}$$

of the optimal parameters and convergence rates with respect to the mesh size h is known for quite general domains, see [9]. Now, if we investigate the asymptotics of the optimal parameters and rates in the nonlinear case II, displayed in Figure 7, with respect to h, we find

$$\gamma_{opt} = \mathcal{O}(h^{-0.45}) \quad \text{and} \quad \rho_{opt} = 1 - \mathcal{O}(h^{0.44})\,. \tag{28}$$

Thus, we do not only observe an asymptotic behaviour of a similar kind as in the linear case, but even with similar exponents. The situation for Case I is virtually the same.

The convergence speed of the Robin method can be further increased by allowing the Robin parameters γ_1 and γ_2 to be different. We have carried out extensive numerical parameter studies for the performance of the nonlinear Robin method in both our cases on levels 1 to 8. Figures 9 and 10 shall serve as examples of the results we obtained on the 4th level in Case I (with 34,000 parameter pairs) and in Case II (with 77,000 parameter pairs), respectively. First of all, in both graphics, which contain the case $\gamma = \gamma_1 = \gamma_2$ on the diagonal, one can clearly see that the convergence speed can be increased by an appropriate choice of different Robin parameters.

Now, however, the situations in Case I and in Case II are completely different. We start by considering Case I, where the slopes of the nonlinearities in the subdomains are different but not their order of magnitude. Here, we observe that the convergence rates are nearly symmetric with respect to the diagonal $\gamma_1 = \gamma_2$ and that two local minima occur off the diagonal—a left (asymptotically global) one and a right one in Figure 9. Although the convergence speed can be increased by choosing different instead of equal Robin parameters, asymptotically we still obtain degenerating optimal parameters

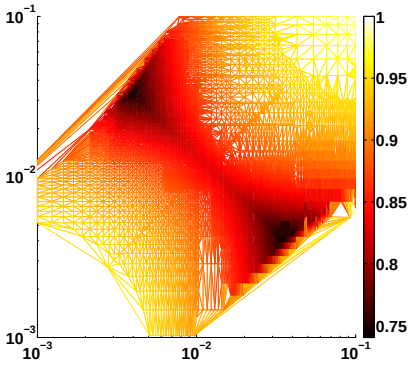

Fig. 9. ρ vs. γ_1 (x-axis) and γ_2 (y-axis) on level 4 for Case I

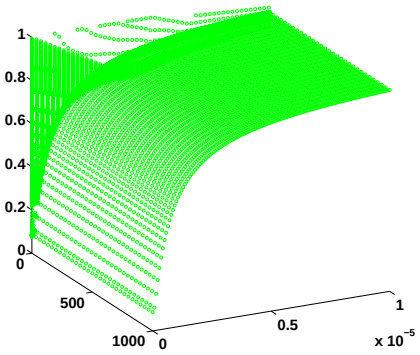

Fig. 10. ρ vs. γ_1 (x-axis) and γ_2 (y-axis) on level 4 for Case II

and rates. However, we observe a weaker mesh-dependence of the convergence rates than for $\gamma_1 = \gamma_2$ in (28). Concretely, we find the asymptotic behaviour

$$\gamma_{1,opt} = \mathcal{O}(h^{-0.37}), \quad \gamma_{2,opt} = \mathcal{O}(h^{-0.55}) \quad \text{and} \quad \rho_{opt} = 1 - \mathcal{O}(h^{0.34}) \tag{29}$$

for the left minima and a similar one for the right minima.

As before in (27), our observations (29) in the nonlinear case I can be compared to known results from the linear theory of optimized Schwarz methods. In [7, p. 17] the asymptotic behaviour of different optimized Robin parameters and corresponding convergence rates has been derived for a linear equation on $\mathbb{R}^2$ decomposed into two half planes. The asymptotics is given by the formulas

$$\gamma_{1,opt}^{lin} = \mathcal{O}(h^{-1/4}), \quad \gamma_{2,opt}^{lin} = \mathcal{O}(h^{-1/4}) \quad \text{and} \quad \rho_{opt}^{lin} = 1 - \mathcal{O}(h^{1/4}). \tag{30}$$

A comparison with (30) shows that, quantitatively, the asymptotic behaviour of the different optimal Robin parameters in (29) does not seem to follow the linear results. Also, we do not obtain the same degree of acceleration of the convergence speed in (29) as suggested by the linear case. However, we observe a similar kind of asymptotic behaviour for ρ_{opt} and, at least, the asymptotics lies between the situations (27) and (30).

In contrast to Case I, the situation in Case II is very unsymmetric with respect to the diagonal $\gamma_1 = \gamma_2$, and we do no longer observe two distinct local minima of convergence rates. We rather have a whole strip of parameter pairs, where one parameter γ_2 is more or less fixed while the other γ_1 is free (as long as it is big enough), in which nearly constant globally minimal rates occur. Even for the global minimum, which is not distinct, one observes a difference in order of magnitude of at least $\gamma_{1,opt} \approx 10^4\, \gamma_{2,opt}$ on levels 1 to 8. Most importantly, however, the globally minimal rates in the strip are asymptotically stable, i.e., mesh-independent. This can be seen in Figure 8, where the value for the 7th level is the same as for the 8th level. Note that with

extreme values $\gamma_{1,opt} \gg \gamma_{2,opt}$ subproblems (20)–(21) and (22)–(23) resemble Dirichlet and Neumann problems, respectively, i.e. the Robin method becomes an undamped Dirichlet–Neumann method. This observation is quite striking if we compare Figure 8 for the optimized Robin method with two different parameters with Figure 6, which shows the optimal convergence rates for the damped Dirichlet–Neumann method.

We close this section by mentioning a known result on the Robin method applied to a linear equation with discontinuous coefficients $K_1/K_2 < 1$ in $\mathbb{R}^2$, decomposed into two half planes, see [5, p. 84]. The asymptotic behaviour in this case is given by

$$\gamma_{1,opt}^{lin} = \mathcal{O}(1)\,, \quad \gamma_{2,opt}^{lin} = \mathcal{O}(h^{-1}) \quad \text{and} \quad \rho_{opt}^{lin} = \frac{K_1}{K_2} - \mathcal{O}(h^{1/2})\,. \tag{31}$$

Although, again, we cannot confirm the asymptotic behaviour for the optimized Robin parameters in our Case II, this rare result of a mesh-independent convergence rate for the Robin method makes our findings in this and in the previous section on the good convergence of our optimized methods in Case II a bit more understandable.

References

1. H. Berninger. *Domain Decomposition Methods for Elliptic Problems with Jumping Nonlinearities and Application to the Richards Equation*. PhD thesis, 2007.
2. H. Berninger. Non-overlapping domain decomposition for the Richards equation via superposition operators. In *Dom. Decomp. Meth. in Sc. and Engin. XVIII*, volume 70 of *LNCSE*, pages 169–176. Springer, 2009.
3. H. Berninger, R. Kornhuber, and O. Sander. On nonlinear Dirichlet–Neumann algorithms for jumping nonlinearities. In *Dom. Decomp. Meth. in Sc. and Engin. XVI*, volume 55 of *LNCSE*, pages 483–490. Springer, 2007.
4. M. Discacciati. *Domain Decomposition Methods for the Coupling of Surface and Groundwater Flows*. PhD thesis, 2004.
5. O. Dubois. *Optimized Schwarz Methods for the Advection-Diffusion Equation and for Problems with Discontinuous Coefficients*. PhD thesis, 2007.
6. P. Bastian et. al. A generic grid interface for parallel and adaptive scientific computing. Part II: Implementation and tests in DUNE. *Computing*, 82(2-3):121–138, 2008.
7. M.J. Gander. Optimized Schwarz methods. *SIAM J. Numer. Anal.*, 44(2):699–731, 2006.
8. P.L. Lions. On the Schwarz alternating method. III: A variant for nonoverlapping subdomains. In *Dom. Decomp. Meth. for Part. Diff. Eq., Proc. 3rd Int. Symp.*, pages 202–223. SIAM, 1990.
9. S.H. Lui. A Lions non-overlapping domain decomposition method for domains with an arbitrary interface. *IMA J. Numer. Anal.*, 29(2):332–349, 2009.
10. A. Quarteroni and A. Valli. *Domain Decomposition Methods for Partial Differential Equations*. Oxford Science Publications, 1999.